

15-10-2003

## Accelerated iterative blind deconvolution of still images

Prashan Premaratne

*University of Wollongong*, prashan@uow.edu.au

M. Premaratne

*University of Wollongong*

Follow this and additional works at: <https://ro.uow.edu.au/engpapers>



Part of the [Engineering Commons](#)

<https://ro.uow.edu.au/engpapers/46>

---

### Recommended Citation

Premaratne, Prashan and Premaratne, M.: Accelerated iterative blind deconvolution of still images 2003.  
<https://ro.uow.edu.au/engpapers/46>

Research Online is the open access institutional repository for the University of Wollongong. For further information contact the UOW Library: [research-pubs@uow.edu.au](mailto:research-pubs@uow.edu.au)

# Accelerated Iterative Blind Deconvolution of Still Images

Prashan Premaratne<sup>1</sup> and Malin Premaratne<sup>2</sup>

<sup>1</sup> School of Electrical, Computer & Telecommunications Engineering,  
The University of Wollongong, Wollongong, NSW Australia 2500.  
prashan@uow.edu.au

<sup>2</sup> Centre for Telecommunications and Information Engineering  
Department of Electrical and Computer Systems Engineering  
Monash University, Clayton, Victoria, Australia 3800.

**Abstract**— We propose an approach for blind deconvolution of still images with moderate noise contamination. The iterative technique is based on the general concepts of iterative techniques for blind deconvolution. The ill-convergence problem associated with most of the iterative techniques is circumvented in our approach using zero-sheet separation techniques. This technique can handle real images blurred by complex Point Spread Functions (PSF), which is a common imaging problem, with Blur Signal-to-Noise Ratios (BSNR) of 70dB and above for PSF of size 32x32 and larger. The technique performs much better for PSFs of smaller sizes with low BSNR around 30dB and provides convergence of the final solution with minimum iterations and is also capable of determining the size of the PSF.

## 1. INTRODUCTION

The well-publicized developments in Hubble Space Telescope and the Mars Pathfinder mission have hailed the success of the digital image restoration techniques and have injected enormous motivation for the development of similar technologies. Blind image deconvolution which tries to separate the convolved functions with minimum a priori knowledge about the imaging system as well as the original image shows much promise for future, as space exploration success becomes a part of day to day life similar to communications revolution. The recent revelation of possible water seepage on Mars may expedite the quest for greater space exploration. Reliable and fast algorithms for blind image restoration are essential for planning and coordination of these future missions.

Ayers and Dainty (AD) [1], pointed out that blind deconvolution is possible with iterative steps starting with initial random estimations for both PSF and true image. However, their approach often failed to obtain a stable final solution. Moreover, an uncertain result arising from much computational burden is certainly not justified. Davey et al. [2], also have reported the success of a variation of Ayers and Dainty method, which could deconvolve single complex

images. Miura et al. [3] reported some success in deconvolving astronomical speckle images when multiple frames are available from the same object(s). However, many frames in the order of 10 were needed for a successful restoration of speckle images. We also have previously reported successful deconvolution of blurred images with symmetric PSFs [4].

This proposed algorithm is shown to be able to cope with most of the shortcomings of the existing algorithms, specially the uncertainty in the convergence of the final result. The algorithm is attractive since it only requires one blurred image. Our technique is specifically targeted at coherent imagery, as this is a practical situation arises in photography related to space exploration. Although our technique is very much resilient to noise contamination amounting to 30dB for smaller PSF of sizes 3x3 to 5x5, providing excellent restorations, we are only presenting simulation results for the much difficult larger PSFs of size exceeding 32x32. We expect that this approach would result in more practical usage of our research. Moreover, this research provides a low computationally complex approach and is able to handle very large images and PSFs unlike the failures associated with the original zero-sheet separation techniques initiated by Lane et al., [5]. Furthermore, it is robust for moderate amount of noise. An added advantage of our technique is that it can determine the size of the PSF and consequently the true image size even in the presence of noise. Furthermore, in the absence of noise, the PSF recovery is highly accurate and the true image can be obtained in a single iteration. The simulation results at the end of this article describe an example, which illustrate the versatility of the proposed method.

## 2. THEORETICAL DEVELOPMENT

Let the true (original) image be denoted by  $f(x,y)$ , the common PSF be given by  $h(x,y)$  and the blurred image is denoted by  $g(x,y)$ . The blurring process can be expressed as

$$g(x, y) = f(x, y) * h(x, y) + n(x, y), \quad 0 \leq x, y \leq N + M - 2. \quad (1)$$

where  $n(x, y)$  denotes additive Gaussian noise in the system,  $*$  denotes 2-D convolution operator and the true images are of size  $N \times N$  and PSF is of size  $M \times M$ . Since we assume the mean value of the true image is preserved in the degradation process the following expression holds,

$$\left| \sum_{(l, m) \in R_h} h(l, m) \right| = 1, \quad (2)$$

where  $R_h$  is the support size of the PSF. If we allow the upper case letters represent the 2-D Discrete Fourier Transform (DFT) of their lower case counterparts and BSNR is high such that we can ignore noise terms

$$G(k, l) = F(k, l)H(k, l), \quad 0 \leq k, l \leq N + M - 2. \quad (3)$$

In this algorithm, initial estimate of the PSF is obtained using the concepts of zero sheet separation as discussed in next section. Assuming that an initial estimate of the PSF is available and the blurred images are corrupted with moderate amount of noise, we outline the next steps involved in the algorithm as follows.

The basic structure of the algorithm is presented in Fig. 1. The image estimate is denoted by  $\hat{f}(x, y)$  and the capital letters represent fast-Fourier transformed (FFT) versions of the corresponding signals. Subscripts denote the iteration number of the algorithm.

Using the initial estimate of FFT of PSF,  $\hat{H}(u, v)$ , obtained as described in section 3, an initial estimate of the true image is calculated using the following recursive formula (Fourier constraint I in Fig. 1) [6]

$$\hat{F}_1(u, v) \approx \left[ \frac{1}{\hat{H}(u, v) |\hat{H}(u, v)|^2 + K} \right] G(u, v), \quad (4)$$

where  $K$  denotes a constant which approximates the noise-to-signal power ratio. This can be arbitrarily chosen as this information may not be available in blind deconvolution scenario. After the initial estimate of the original image, successive estimates are calculated using the following incremental Wiener-type filter (Fourier constraint II in Fig. 1) [6].

$$\hat{F}_k(u, v) = \frac{G(u, v) \hat{H}_{k-1}^*(u, v)}{|\hat{H}_{k-1}(u, v)|^2 + \alpha / |\hat{F}_{k-1}(u, v)|^2} \quad (5)$$

where  $(.)^*$  denotes the complex conjugate of  $(.)$ . The real constant  $\alpha$  represents the energy of the additive noise and is determined by prior knowledge of the noise contamination level, if available. Since the algorithm is targeted at restoration of gray scale images, the intensity levels are distributed in a range from 0-1. Any negative values or positive values above this range are supposed to saturate the image sensor and hence could be used as a *spatial domain constraint* for the estimated image. Hence, the initial estimate of the image calculated from Eq. (4) is used in Eq. (5) for evaluating successive iterations of the true image using the following constraint

$$\hat{f}(x, y) = \begin{cases} 1, & \hat{f}(x, y) > 1 \\ 0, & \hat{f}(x, y) < 0 \\ \hat{f}(x, y), & 0 \leq \hat{f}(x, y) \leq 1 \end{cases} \quad (6)$$

The restoration is always guaranteed to converge, since a good estimate of the PSF is available through zero-sheet separation. Even though, we do not provide an analytical proof of the convergence, it can be argued that zero sheet separation provides best estimate of PSF for any given amount of noise contamination. The algorithm is usually run till a visually appealing image emerges. In most of the cases, restoration converges in a few iterations.

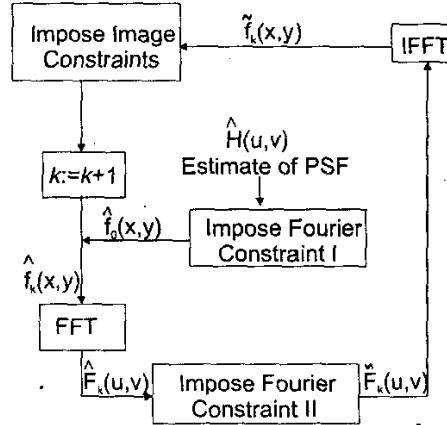


Fig. 1 Schematic Diagram of Proposed Scheme

### 3. SIMULATION RESULTS

For the simulation results, we initially used well-known gray-scale image of the 'cameraman'. Even though, this image is of size 256x256, we cropped it to the size of 250x250 as shown in Fig. 2. This was to produce a degraded image of size 256x256 as a result of the convolution with the PSF of size 7x7 (image of size 250x250 when convolved with a PSF size 7x7 produces a convolution of size

256x256). The PSF complies with Eq. (2) to preserve the mean value during the degradation and the blurred image with noise contamination amounting to (Blur Signal to Noise Ratio) BSNR of 30dB is shown in Fig. 3.



Fig. 2. Original 'Cameraman' Image



Fig. 3. Degraded Image with BSNR of 30dB.

**Table 1** Summary of the zero sheet Separation for the retrieval of PSF in proposed Iterative Blind Restoration. Assume a real image blurred by a complex PSF with additive white Gaussian noise with BSNR of 70dB or above.

1. Support size of the PSF is evaluated [4].

2. Generate the relevant rows of the zero-sheet (each row contains zeros of both PSF and true image).
3. Using a search mechanism all zeros appearing as complex conjugate pairs (even though, they are present in different rows) are removed [4].
4. Now only PSF zeros and a few *real* zeros that might be belonging to true image remain in each row. Remove any real zeros that might be in excess of the PSF support size ( $M-1$ ).
5. Build one-dimensional polynomials for each row. The size of the PSF now is  $M \times M$ .
6. Multiply each column by a suitable column vector (this vector has variable elements which will be determined later).
7. Steps 2-6 are repeated for rows and columns interchanged. This will yield another DFT version of the PSF.
8. Above generated functions are equated and any  $2M-1$  equations are solved to evaluate all unknowns. Thus the DFT of PSF or PSF in spatial domain can be restored (however, noise may reduce the accuracy of these values).

The PSF is recovered using the zero sheet separation techniques as described in [4] (The summary of this process is outlined in Table 1). Once the PSF is successfully recovered, this is used in our iterative process as depicted in Fig 1. The image is recovered in about 6 iterations in about 100 seconds using a 400MHz PC Workstation with main memory of 128Mb. We used an ordinary PC to simulate our experiments, as they would be comparable to the powerful workstations used by early researchers a decade ago. Another reason is to point out that our algorithms are computationally inexpensive. However, it has to be pointed out that the bulk of the processing time involved in our experiments was spent on recovering the PSF using zero sheets. This roughly amounted to 20 minutes in our workstation.

**Table 2.** Original 7x7 PSF

-0.1786	0.1071	-0.0714	-0.5714	-0.6071	0.2857	-0.4643
-0.7143	0.1429	0.0357	0.3214	0.2500	0.5000	0.6871
0.0714	0.0714	0.4643	0.6786	-0.1786	-0.5000	-0.3571
0.1071	-0.0714	0.0357	-0.2857	0.2857	0.2300	0.2143
-0.5000	0.3214	-0.0357	0.3571	0.3571	-0.0714	0.1071
0.5000	-0.2500	-0.3571	0.2300	0.3214	-0.6786	-0.3929
0.5000	0.9286	0.1429	-0.6786	0.5357	0.1071	-0.9286

**Table 3.** Recovered PSF from the Blurred Image Contaminated with BSNR of 30dB

-0.1796	0.1136	-0.1032	-0.5618	-0.6818	0.2893	-0.4628
-0.7214	0.1258	0.0430	0.3171	0.2745	0.5040	0.5964
0.0818	0.0711	0.4795	0.6722	-0.1845	-0.5171	-0.3666
0.1157	-0.0722	0.0481	-0.2987	0.2963	0.2174	0.2218
-0.4713	0.3214	-0.0259	0.3321	0.3707	-0.0531	0.0910
0.5100	-0.2554	-0.3565	0.2260	0.3374	-0.6808	-0.3796
0.4891	0.9471	0.1543	-0.6766	0.5189	0.1138	-0.9189

The recovered PSF matrix as shown in Table 3, deviates from the original PSF matrix (shown in Table 2) by about 3% (the matrix elements differ by 3%). However, this difference does not pose any difficulty and the recovery process produces a good estimate to the original as can be seen in Fig. 4. Since the recovery process is very convenient at 50 and 60dB for small PSFs similar to what we used, these results are not presented. However, the more interesting cases arises at large complex PSFs around 32x32. It is well known that many PSFs concerned in coherent imagery are encountered in space imagery are around this size.



Fig. 4. Recovered Image

We used a 32x32 sized complex PSF to degrade For a large PSF as above we have determined that the technique works for moderate noise amounts around 70dB.

Fig. 5 and 6 show the original image and the blurred noisy image with BSNR of 70dB. The recovered PSF may differ from the original PSF by a multiplicative complex constant and is normalized to comply with Eq. (2). The recovered image after 8 iterations is shown in Fig. 7. Even though the restored image is 256x256, only 225x225 size original image resides in the recovered image. This is evident as visible dark edges to the lower and the right sides of the images (Fig. 4 and Fig. 7) due to the removal of the PSF after deconvolution.

Mean Squared Error (MSE) criterion can be used to evaluate the speed of convergence of the final result. Due to historical reasons and popularity, it is more appropriate to use a standardized MSE, which is denoted as follows

$$\text{MSE}(\hat{f}) = \frac{\sum_{x,y} [a\hat{f}(x,y) - f(x,y)]^2}{\sum_{x,y} f^2(x,y)} \quad (7)$$

Because of the constraint imposed by Eq. (2) we expect constant  $a$  in the above expression to assume a value around 1 minimizing MSE. Fig. 8 shows MSE values against the iteration number for our proposed method. It should be mentioned that this MSE value is obtained with a single evaluation and is not averaged over several runs. The minimum value attained for proposed scheme was less than 0.38.



Fig. 5. Original Image of Lenna

It has to be mentioned that as the MSE criteria does not adequately represent the local image improvements, the MSE value attained in the convergence is more pleasing than the restoration achieved with the MSE. In our simulation, we achieved a MSE value of 0.377 at the end of two iterations although the restoration converged to a more stable MSE value of 0.38 only after 5 iterations. The constraint imposed on the image by Eq. (6) attempts guarantee the image pixels are positive even though, this result in higher MSE. The proposed technique yielded the exact PSF for noiseless case. Although we have done our best to incorporate noise amounting to BSNR of 70dB for moderate-sized PSFs (32x32), the technique may not perform well for lower BSNRs for larger PSFs. However, we observed better performance for smaller PSF at lower BSNRs. This technique is not applicable to complex images as the zero-sheet separation relies on removal of complex conjugate zeros. Any complex image would not contain complex conjugate pairs of zeros and would be impossible to separate. In future, we plan to investigate the possibility of extending this algorithm for complex images for lower BSNRs.

#### 4. CONCLUSIONS

We reported a novel technique with superior convergence performance for iterative blind deconvolution of still images with moderate noise contamination. The main attractiveness of the reported method is its ability to restore moderate-sized images (512x512) without significant computational overhead compared with existing similar algorithms. We showed, by using a close estimate of the point spread function as the initial estimate, successful iterative restoration of an image corrupted with BSNR of 70dB for moderate-sized PSFs (32x32). We also demonstrated the applicability of the proposed restoration algorithm for smaller PSF with low BSNRs.



Fig. 6: Blurred Image with Noise of 70dB



Fig. 7: Recovered Image

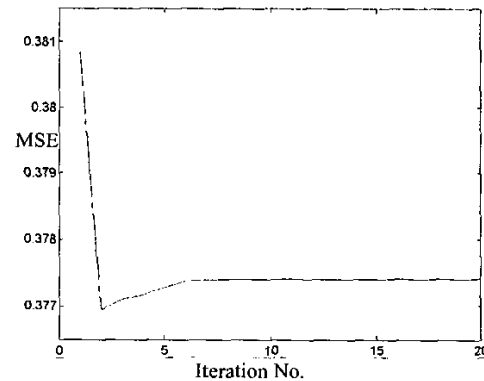


Fig. 8: MSE for Different Iterations

#### REFERENCES

- [1] G. R. Ayers, J. C. Dainty, "Iterative Blind Deconvolution Method and Its Applications", *Optics Letters* 13-7, 547-549, 1988.
- [2] B.L.K. Davey, R.G. Lane, R.H.T. Bates, "Blind Deconvolution of Noisy Complex Valued Images", *Opt. Commun.* 69-5,6, 353-356, 1989.
- [3] N. Miura, N. Baba, "Extended-Object Reconstruction With Sequential Use Of The Iterative Blind Deconvolution Method" *Opt. Commun.* 89, 375-379, 1992.
- [4] P. Premaratne, C. C. Ko, "Retrieval Of Symmetrical Image Blur Using Zero Sheets", *IEE Procee. Vision, Image and Signal Processing* 148-1, 65-69, 2001.
- [5] R.G. Lane, R.H.T. Bates, "Automatic Multidimensional Deconvolution" *J. Opt. Soc. Am. A* 4-1, 180-188, 1987.
- [6] R.C. Gonzalez, R.E. Woods, *Digital image processing*, (R.C. Gonzalez, R.E. Woods), 253-300, Addison-Wesley, U.S.A., 1993.